

# The Effect of Cavitation Water Jet Shock as a Newly Technology on Micro-Forming Process

**James Kwasi Quaisie**

Welding and Fabrication Engineering Department, Faculty of Engineering, Tamale Technical University, Ghana  
jkquaisie@tatu.edu.gh  
(corresponding author)

**Philip Yamba**

Mechanical Engineering Department, Faculty of Engineering, Tamale Technical University, Ghana  
pyamba@tatu.edu.gh

**Vitus Mwinteribo Tabie**

Mechanical Engineering Department, Faculty of Engineering, Dr. Hila Liman Technical University, Ghana  
tabieson@yahoo.com

**Joseph Sekyi-Ansah**

Department of Mechanical Engineering, Takoradi Technical University, Ghana  
josephsekyiansah1981@gmail.com

**Anthony Akayeti**

Mechanical Engineering Department, Faculty of Engineering, Tamale Technical University, Ghana  
aanthony@tatu.edu.gh

**Abdul-Hamid Mohammed**

Welding and Fabrication Engineering Department, Faculty of Engineering, Tamale Technical University, Ghana  
zuumham78@gmail.com

*Received: 22 December 2022 | Revised: 11 January 2023 | Accepted: 15 January 2023*

**ABSTRACT**

This article proposes a novel technology called water jet cavitation shock micro-forming to fabricate micro-features on 304 stainless steel foils with a thickness of 100 $\mu$ m, using a cavitation nozzle with an incident pressure of 8 to 20MPa. This study investigated the surface morphology of the formed part, the influence of incident pressure, target distance, and impact time on the forming depth, and an analysis of the punching phenomenon of the formed components. The experimental results after the water jet cavitation shocking indicated that the surface morphology of the formed part of the 304 stainless foil sample had good quality and no conventional defects such as die scratches and cracks. Furthermore, when the incident pressure was 20MPa, the height of the uniform-shaped spherical cap exceeded 262 $\mu$ m. The forming depth increased with increasing incident pressure and impact time. Under an incident pressure of 20MPa, with the increase of target distance, the average depth of the formed part increased at first and then decreased. Finally, the analysis of the blanking phenomenon indicated that when the incident pressure increased to 30MPa, the workpiece was completely blanked. This is mainly because, under this incident pressure, the shockwave pressure generated by the collapse of the bubble deforms the workpiece beyond the stress limit of the material itself.

*Keywords-novel technology; cavitation nozzle; incident pressure; surface morphology; shockwave*

## I. INTRODUCTION

Water jet technology is a cold working method that has been applied to a variety of industries, including civil engineering, architecture, and manufacturing. In this technology, water is discharged from nozzles under big pressure. This technology has been used to investigate water jet flows and develop new usages [1]. Cavitating jet in air [2], multifunction cavitation [3-6], and Water Jet Cavitation (WJC) [7, 8] are some of the available water jet processing methods. This study investigated WJC technology, which involves processing a workpiece surface using a high-speed underwater cavitation jet in a water-filled tank. The impact pressure slightly deforms the material surface layer plastically by generating a restraining force between the lower layers and the surface and causes a peening (forming) effect that increases the pits' depth hardness near the surface and applies compressive residual stress.

Many studies have investigated micro forming using various forms of applications for plastic deformation of metal foil. In [9], a study was conducted on a metallic foil using a micro-energy ultraviolet pulse laser shock for micro-pattern transfer. The experimental results indicated that the depth of the micropattern increased with increasing single pulse energy and the ratio of overlap in a certain range. This revealed that the depth formed of aluminum foil printed on a #400 mold was greater than that in #1000 and more sensitive to the pulse energy and the rate of overlap. In [10], a novel laser shock technology was also used to study the deformation behavior of pure copper foil. The results showed that after each shock, the formed area increased, and, at the same time, the undeformed area decreased until it disappeared. The power density of the laser can be applied to improve the accuracy dimension, surface roughness, and micro-hardness of micro-parts. The impact of the base metal surface roughness and the spread behavior of the bag-8 was studied in [11], and the optimum surface roughness found in Rz was 0.92 [12]. In [13], the degradation of the micro-mold surface was investigated using laser dynamics in forming and its effects on the material. The experimental results showed the avoidance of growth, coalescence, and nucleation under repeated shock loading form surface degradation on micro-mold. Laser shock waves can be used for micro-coining to replicate features on the metal surface. In [14], laser shock hydraulic forming was proved to have a good matching influence and can prevent or even suppress copper foil springback, which is appropriate for forming features of the large-region array. In [15], the punch force behavior was investigated during the micro v-bending of the copper foil. The results indicated that the free-bending and the coin-bending stages were part of the punch force profile. The application of laser technology has been studied extensively and has become more mature and applied to many processes, such as laser welding, laser shock peening, and laser shock forming [16-17].

To the best of our knowledge, there are no reports of metal foil micro-forming using water jet cavitation shock. This paper introduces a new process technology called cavitation water jet shock micro-forming. This process has the advantages of being low-cost, having good processing flexibility, and dramatically

improving formability. The versatility and low cost of water-jet cavitation technology make it superior to conventional micro-forming such as laser micro-forming, which is more expensive, requires high-skill labor, etc. Additionally, as the interface between fabrication tools and the work components is liquid-to-solid, the manufacturing friction is reduced, negating the need for lubrication during the forming process. This study aims to demonstrate the feasibility of this process. Water jet cavitation shock micro-forming is based on high-pressure shocks as a source for the forming energy created through the collapse of cavitation bubbles. During this process, a high-speed jet of water is injected into a water-filled chamber, and cavitation occurs in the shear layer around the jet. This type of jet is called a cavitation shock water jet. During the process, cavitation bubbles are generated by injecting high-speed water through a nozzle into a chamber filled with water. The cavitation bubbles periodically flow out from the nozzle and spread over the surface of the material to be processed, using the cavitation bubbles generated in the jets as the driving force, and applying high-pressure shock generated by the collapse of the bubbles [18, 19]. In the process of acting on the surface of the material, high-pressure shock waves propagate into the interior of the metal foil.

This study investigated the cavitating water jet shock micro-forming technique to examine the processing parameters on the surface morphology of the formed part, the effect of incident pressure, impact time, and target on forming depth, and analyze the blanking phenomenon using 304 stainless steel foil.

## II. FORMING MECHANISM AND ITS APPARATUS

As illustrated in Figure 1, the typical application of the water jet cavitation shock micro-forming system is mainly composed of a jet-generating device and a forming device. The incident pressure drives the flow of water at a high speed through the cavitation nozzle, aggregation occurs when there is a large number of cavitation nuclei, the low-pressure region inside and outside the cavitation nozzle develops, and finally, the high-velocity liquid flow forms cavitation bubble groups. Adjusting the standoff distance, when the cavitation bubble groups approach the surface of the sample, the environmental pressure around the cavitation bubble groups is suddenly increased due to the huge turbulent pressure pulsation causing the collapse of the cavitation bubble groups and releasing the high-pressure shocks (cavitation bubbles collapse loads) at the moment of collapse [20, 21]. These high-pressure shocks act on the surface of the material and propagate into its interior, while, due to the high concentration of energy [22-24], they are confined to a very small area, and when the peak value of the collapse pressure exceeds the Hugoniot Elastic Limit (HEL) of the material, the metal foil is yielded and plastically deformed. The peak stress of the shock wave decreases as the shock wave propagates deeper into the metal foil. The plastic deformation of the metal foil continues until the peak stress falls below the dynamic yield strength. Since the loading direction is downward and the metal foil is free at the bottom side, the metal foil will bend downward and fill the die.

The forming device is installed on the platform. The quality of the initial interface between the metal foil and the micro-die

is very crucial, so the two surfaces should be attached and bonded to each other. The forming device consists of a locking block, mask, seal ring, metal foils, and micro-die. At the initial stage, the foil was placed on the top of the die, completely covering its openings. The metallic foil flatness should be guaranteed during the process. Next, the mask is placed on the foil and the micro-die had the same axial hole at the center. Finally, the initial contact between the foil and the micro-die is very important, therefore, the two surfaces were firmly locked by a locking block to prevent material wrinkling. In addition, a seal ring was also applied between the foil and the mask to ensure effective sealing.

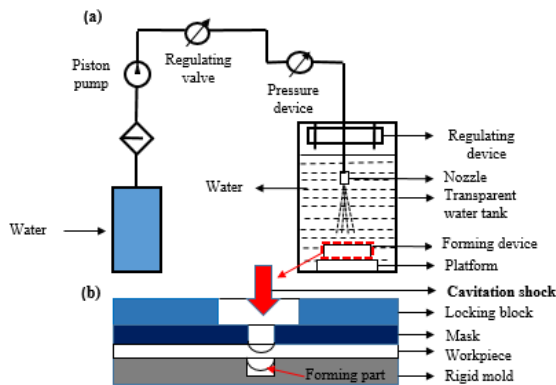


Fig. 1. (a) The formation system of water jets cavitation shock micro-forming and (b) forming device.

III. MATERIALS AND METHODS

A. Material

This study used 304 stainless steel foils due to their technical and economic advantages, as they are widely used in a variety of industrial applications, especially in the manufacture of micro-device components. These steel foils have good processing properties, high durability, good thermal conductivity, high temperature, corrosion resistance, good workability, need little maintenance, are nonmagnetic, are easy to weld and shape, and are completely recyclable (100%). Tables I and II show the chemical composition and the mechanical properties of the 304 stainless steel, respectively. The 304 stainless steel foil samples having 100µm thickness were cut into 50×50mm square specimens. The square samples were cleaned from dirt with anhydrous alcohol and the residual liquid was wiped off the surface.

TABLE I. CHEMICAL COMPOSITION OF 304 STAINLESS STEEL

Element	C	Mn	P	S	Si	Cr	Ni
Wt (%)	≤ 0.8	≤ 2.0	≤ 0.045	≤ 0.03	≤ 1.0	≤ 18.0	≤ 8.0

TABLE II. MECHANICAL PROPERTIES OF 304 STAINLESS STEEL

Elastic modulus (GPa)	Poisson ratio	Yield strength (MPa)	Tensile strength (MPa)	Extension rate (%)
194	0.3	≥ 205	≥ 520	≤ 40

B. Experimental Setup

Figure 2(a) shows a schematic diagram of the experimental setup of the water jet cavitation shock micro-forming equipment used for the process. Tap water was stored for at least 24 hours before the experimental test in a large tank of 2.5×2×1.5m at a room temperature of 25±2°C. A transparent water tank with a square horizontal cross-sectional area of 500×500×900mm was used to carry out the experiments. For transparent flow purposes, the tank was made of acrylic resin. The nozzle used in this experiment was designed regarding the angular nozzle for producing the periodic behavior of the jets of cavitation as shown in Figure 2(b) [25]. The nozzle was fixed in water at room temperature. The pumped water was discharged at an incident pressure of 8-20MPa. The throat nozzle diameter was 1.5mm and the throat length *L* was 12mm with an expansion angle *θ* of 30°. The optimal nozzle size ratio was *d*:*L*=1:8 [26]. The distance between the sample workpiece was 120mm. Inside the test cell, the sample was placed perpendicularly to the cavitating jets. The axial distance *S<sub>L</sub>* between the micro-die cavity and the jet axis was fixed at 10mm (the eccentricity *S<sub>L</sub>* was 10mm). Pressure was attached to the nozzle through the inflow hole. A duration time of 120s was selected for this experiment with incident pressures of 8, 12, 16, and 20MPa.

According to (1), the cavitation number is a measure of the flow's resistance to cavitation and is roughly equal to the ratio of the incident (upstream) to downstream pressures.

$$\sigma = \frac{p_1}{p_2} \tag{1}$$

In this instance, *p<sub>1</sub>* denotes the incident pressure and *p<sub>2</sub>* denotes the downstream pressure. Incident pressure is one of the crucial factors in the process of water-jet cavitation shock micro-forming. The downstream pressure *p<sub>2</sub>* was maintained at 0.1MPa, while the incident pressure *p<sub>1</sub>* was set to 8, 12, 16, and 20MPa [19], resulting in cavitation numbers of 0.0125, 0.0083, 0.0063, and 0.005, respectively.

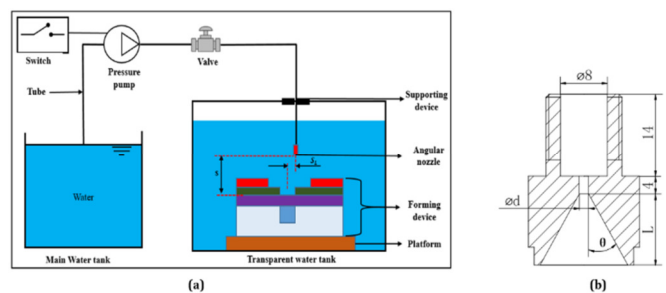


Fig. 2. (a) Experimental system of water jets cavitation shock micro-forming, (b) nozzle geometry diagram.

C. Forming Device

According to Figure 3, the forming tool includes a locking block, mask, seal ring, workpiece, and micro-die. The top of the die was covered with foil, totally enclosing the die apertures, assuring it was flat. The mask was then positioned on the foil with the identical axial hole in the center as the micro-die. The initial interface between the foil and the micro-die is

particularly important for preventing material wrinkling, hence, the two surfaces should be firmly linked to one another by a locking block. In addition, a seal ring was placed between the mask and the foil to provide an efficient seal.



Fig. 3. The forming device.

#### IV. RESULTS AND DISCUSSION

This section presents the results of the surface morphology of the formed part, the influence of incident pressure on forming depth, the influence of impact time on forming depth, the effect of target distance on forming depth, and an analysis of the punching phenomenon.

##### A. Surface Morphology of Formed Part

In the process of metal foil micro-forming, a good forming effect can be obtained by selecting the appropriate process parameters [27]. A 304 stainless steel foil with a size of 50×50mm was selected for micro-forming experiments. Figure 4 shows the 304 stainless steel foil at incident pressure of 20MPa, target distance of 120mm, impact time of 2min, and eccentricity of 14mm. Figure 4(a) shows that the finished surface of the 304 stainless steel foil-formed parts was better than the surrounding unformed parts and had better outline shape and surface quality. In addition, it was observed that the edge of the formed part had no wrinkles, fractures, or other phenomena, indicating a better surface quality than the traditional micro-forming method [28].

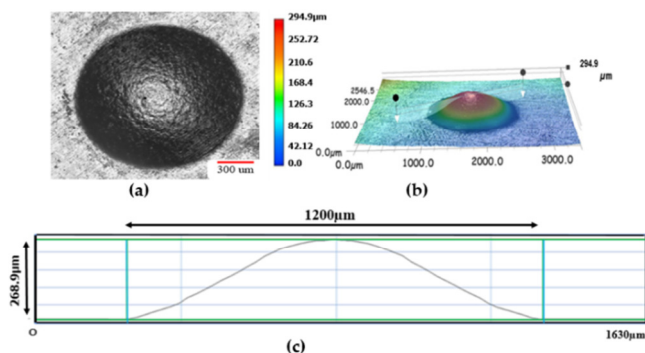


Fig. 4. (a) Micro-formed sample, (b) 3D surface morphology of formed parts, and (c) section profile curve of formed parts.

Figure 4(b) shows that the 304 stainless steel foil obtained a good geometric shape during this forming process. The center area of the formed part has the darkest color, indicating that a

strong plastic deformation occurred during the process. Around it, the color gradually becomes lighter and the amount of deformation gradually decreases. Figure 4(c) shows the typical cross-sectional profile curve of the micro-formed part. Its cross-sectional shape is like a "spherical coronal cone" with a diameter of 1.2mm. In addition, the cross-sectional curve of the formed part had a smooth profile, without abrupt changes, and a good forming effect, which indicates that the material flows into the die uniformly during the forming process. The maximum forming depth of the formed part was 268.9μm.

##### B. Effect of Incident Pressure on Forming Depth

In the experiment of cavitation water jet shock metal foil micro-forming, the forming depth of the foil can be an evaluation index of its forming quality. The incident pressure is one of the key parameters of the cavitation water jet shock micro-forming experiment, so it is necessary to analyze its effect on the deformation of the foil. To make the test results comparable, the other process parameters were fixed and only incident pressure was adjusted to 8, 12, 16, and 20MPa. The target distance was 120mm, the impact time was also 2min, and the eccentricity was 14mm. The results showed that when the incident pressure was 8, 12, 16, and 20MPa, the corresponding average forming depths were 89.2, 145.9, 169.9, and 226.6μm, respectively. Figure 5 shows the variation in the forming depth. This indicates that the plastic deformation of the 304 stainless steel foil increased non-linearly with incident pressure [29]. The forming depth improved at a decreasing rate when the incident pressures increased from 8 to 16MPa and increased sharply when the incident pressures changed from 16 to 20MPa. This could be attributed to the following reasons:

- When the incident pressure is less than 16MPa, the cavitation bubbles mostly collapse before reaching the material surface under the standoff distance of 120mm, hence, the shock energy was relatively low and the improvement of the forming depth was not high. Although the cavitation bubbles have a larger size and collapse on the material surface, they produce greater shock energy which increases the forming depth sharply when the incident pressure increased to 20MPa.
- The dynamic yield limit of the material increases due to the residual stress and the hardened effect during the shock-forming process. Therefore, a stronger force is needed to produce continued deformation.

##### C. Effect of Target Distance on Forming Depth

Incident pressure was set to 20MPa, impact time was set to 2min, and eccentricity to 14mm and the influence of target distance (80, 100, 120, and 140mm) on the forming depth was studied. The depth was measured and its average value was calculated. Figure 6 shows the average depth curve of 304 stainless steel foil-formed parts at different target distances. Under an incident pressure of 20MPa, with increasing target distance, the average depth of the formed part increases first and then decreases. When the target distance was 120mm, the average depth of the formed part was the largest, reaching 226.6μm. This was mainly due to the increase in the target distance that increased the shockwave pressure acting on the workpiece surface. However, with an increasing target

distance, most of the cavitation bubbles collapse before reaching the surface of the workpiece, so the impact energy was relatively low as the depth increased.

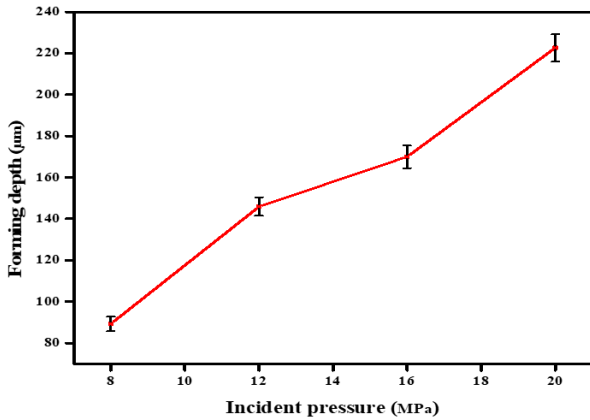


Fig. 5. The maximum depth with different incident pressures.

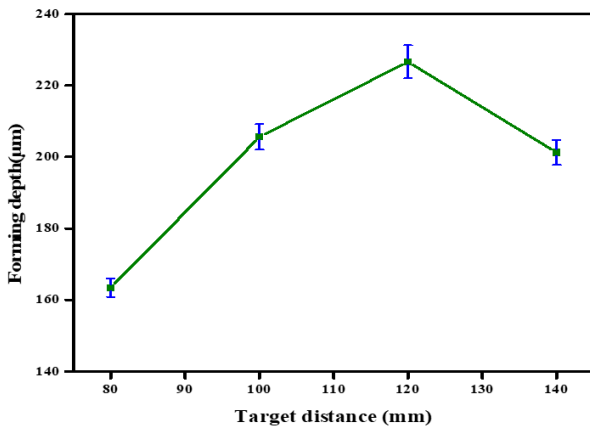


Fig. 6. The average depth depending on different target distances.

D. Effect of Impact Time on Forming Depth

To investigate the influence of impact time on the forming depth of the 304 stainless steel foil, the incident pressure was 8, 12, 16, and 20 MPa, the target distance was 120mm, the eccentricity was fixed at 14mm, and the impact time was 40, 80, 120, and 160s, respectively. Figure 7 shows that under the same incident pressure (8 MPa), the average forming depth of the formed part increased nonlinearly with increasing impact time. With an incident pressure of 8MPa, when the impact time increased from 40 to 160s, the forming depth increased from 40.4µm to 116.1µm, which is almost three times the initial value. However, with increasing time, the growth rate of forming depth gradually decreased. When the incident pressure increased from 12 to 16MPa, the change in the average forming depth followed the same trend. In addition, when the incident pressure was 20MPa, forming depth increased from 91.8µm at 40s impact time to 252.7µm at 160s, which is also approximately a three-time increase. These results show that the incident pressure and the impact time directly determine the forming effect of the metal foil. In addition, it was found that in the subsequent impact process of the cavitation water jet, the

growth rate of the forming depth of the material gradually reduced. This can be attributed to the fact that as the entire forming device was placed in water, the forming depth also increased with increasing impact time. Furthermore, since it is difficult to achieve complete sealing, a small amount of tap water will flow into the pit, thereby gradually reducing the impact effect.

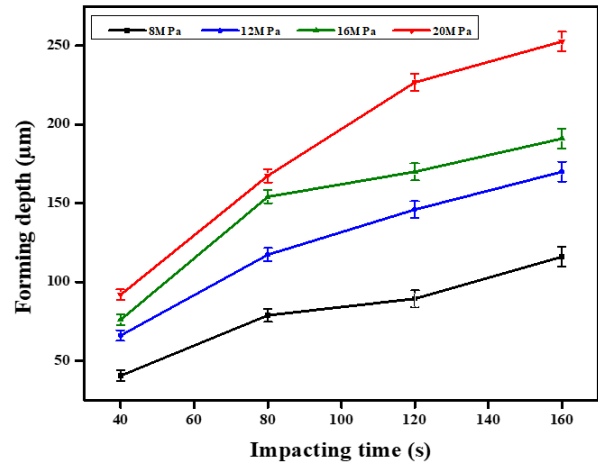


Fig. 7. The average forming depth depending on different impact times.

E. Analysis of the Blanking Phenomenon

In the micro-forming process of metal foil impact by cavitation water jet, the analysis of the causes of material failure and the mechanism behind it helps to understand the impact process conditions and improve the forming quality of the material. In high-speed impact, the material is damaged by crack initiation and propagation, but when cavitation collapses, shockwave and inertia act on the target and at the same time a variety of damages such as adiabatic shear instability, breakage, and spallation would also occur. When the target distance was 120mm, the eccentricity was 14mm, and the incident pressure exceeded a certain value, the foil had a severe shear effect and a cut-off at the edge of the die. Figure 8 shows the blanking effect of the 304 stainless steel foil under an incident pressure of 30MPa.

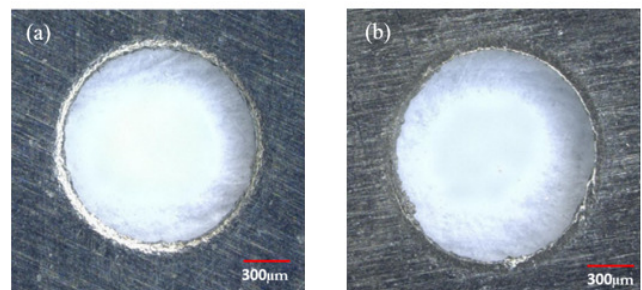


Fig. 8. The morphology of punched hole at the bottom: (a) Front, and (b) reverse side.

Figure 9 shows an SEM image of the back of the punched round hole under the corresponding conditions. When the incident pressure increased to 30MPa, the workpiece was

completely blanked. This is mainly because, under this incident pressure, the shockwave pressure generated by the collapse of the bubble deforms the workpiece beyond the limit stress of the material itself. At the edge of the cavity, the stress value was obtained, which completely exceeds the shear fracture limit of the cavity, leading to the fracture of the material and the complete blanking process.

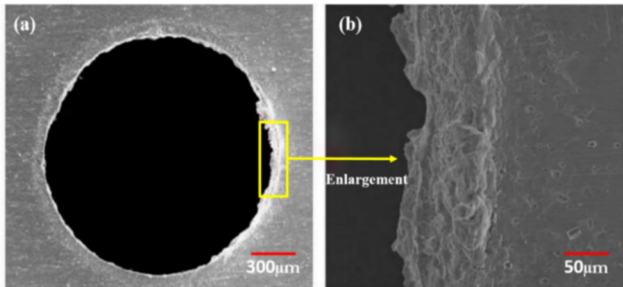


Fig. 9. SEM for punched bottom circle: (a) Whole view, and (b) local magnification view.

## V. CONCLUSION

This study conducted experiments using a cavitation water jet shock micro-forming on a 304 stainless steel foil. The single characteristic micro-forming experiments were carried out, and the impact micro-forming law of the cavitation water jet was analyzed and studied from the aspects of incident pressure, target distance, impact time, and the analysis of the blanking phenomenon. The results showed that the proposed method could obtain micro-formed parts with good surface quality and relatively uniform impact depth formed parts. The forming depth gradually increases with increasing incident pressure and impact time, however, it increases first and then decreases with increasing target distance. In addition, the analysis of the blanking phenomenon showed that when incident pressure continues to increase, there was a risk of cracking at the rounded corners of the micro-formed parts. When the pressure increased to 30MPa, a punch sample of the 304 stainless steel foil of 100µm thickness could be obtained.

## REFERENCES

- [1] M. Ijiri, D. Shimonishi, D. Nakagawa, and T. Yoshimura, "New water jet cavitation technology to increase number and size of cavitation bubbles and its effect on pure Al surface," *International Journal of Lightweight Materials and Manufacture*, vol. 1, no. 1, pp. 12–20, Mar. 2018, <https://doi.org/10.1016/j.ijlmm.2018.03.003>.
- [2] W. Wróblewski, K. Bochon, M. Majkut, E. H. Malekshah, K. Rusin, and M. Stozik, "An experimental/numerical assessment over the influence of the dissolved air on the instantaneous characteristics/shedding frequency of cavitating flow," *Ocean Engineering*, vol. 240, Nov. 2021, Art. no. 109960, <https://doi.org/10.1016/j.oceaneng.2021.109960>.
- [3] M. Ijiri and T. Yoshimura, "Improvement of corrosion resistance of low-alloy steels by resurfacing using multifunction cavitation in water," *IOP Conference Series: Materials Science and Engineering*, vol. 307, no. 1, Oct. 2018, Art. no. 012040, <https://doi.org/10.1088/1757-899X/307/1/012040>.
- [4] Y. Toshihiko, T. Kumiko, and Y. Naoto, "Development of mechanical-electrochemical cavitation technology," *Journal of Jet Flow Engineering*, vol. 32, no. 1, pp. 10–17, Mar. 2016.
- [5] T. Yoshimura, K. Tanaka, and N. Yoshinaga, "Material processing by mechanical-electrochemical cavitation," in *BHR Group 2016 Water Jetting*, Seattle, WA, USA, Nov. 2016, pp. 223–235.
- [6] T. Yoshimura, K. Tanaka, and N. Yoshinaga, "Nano-level Material Processing by Multifunction Cavitation," *Nanoscience & Nanotechnology-Asia*, vol. 8, no. 1, pp. 41–54, Apr. 2018, <https://doi.org/10.2174/2210681206666160922164202>.
- [7] M. Ijiri, D. Shimonishi, D. Nakagawa, and T. Yoshimura, "Evolution of Microstructure from the Surface to the Interior of Cr-Mo Steel by Water Jet Peening," *Materials Sciences and Applications*, vol. 08, no. 10, Sep. 2017, Art. no. 708, <https://doi.org/10.4236/msa.2017.810050>.
- [8] Masataka Ijiri, Daichi Shimonishi, Daisuke Nakagawa, Kumiko Tanaka, and Toshihiko Yoshimura, "Surface Modification of Ni-Cr-Mo Steel by Multifunction Cavitation," *Journal of Materials Science and Engineering A*, vol. 7, no. 6, pp. 290–296, Dec. 2017, <https://doi.org/10.17265/2161-6213/2017.11-12.002>.
- [9] J. Man, H. Yang, H. Liu, K. Liu, and H. Song, "The research of micro pattern transferring on metallic foil via micro-energy ultraviolet pulse laser shock," *Optics & Laser Technology*, vol. 107, pp. 228–238, Nov. 2018, <https://doi.org/10.1016/j.optlastec.2018.05.046>.
- [10] C. Zheng *et al.*, "Laser shock induced incremental forming of pure copper foil and its deformation behavior," *Optics & Laser Technology*, vol. 121, Jan. 2020, Art. no. 105785, <https://doi.org/10.1016/j.optlastec.2019.105785>.
- [11] M. H. Fauzun Tadashi Ariga, "Effect of The Base Metal Surface Roughness on The BAG-8 Spreading Behaviour," *International Journal of Technology*, vol. 2, no. 3, pp. 291–319, Jan. 2014, <https://doi.org/10.14716/ijtech.v2i3.73>.
- [12] I. Alenezi, "Effects of Heat Treatment on the Corrosion Behavior of ASTM A-36 Steel," *Engineering, Technology & Applied Science Research*, vol. 10, no. 1, pp. 5320–5324, Feb. 2020, <https://doi.org/10.48084/etasr.3326>.
- [13] Z. Shen, H. Liu, X. Wang, and C. Wang, "Surface degradation of micro-mold in micro-scale laser dynamic forming and its effects on workpiece," *Optics & Laser Technology*, vol. 117, pp. 114–125, Sep. 2019, <https://doi.org/10.1016/j.optlastec.2019.03.047>.
- [14] H. Liu, C. Jiang, F. Liu, Y. Ma, and X. Wang, "Numerical and experimental investigations of laser shock hydraulic microforming for thin-walled foils," *Thin-Walled Structures*, vol. 143, Oct. 2019, Art. no. 106219, <https://doi.org/10.1016/j.tws.2019.106219>.
- [15] G. Kiswanto, A. Mahmudah, D. Priadi, "Punch Force Behavior during Micro V-Bending Process of the Copper Foil," *International Journal of Technology*, vol. 8, no. 7, pp. 291–319, Dec. 2017, <https://doi.org/10.14716/ijtech.v8i7.747>.
- [16] X. Wang *et al.*, "Micro scale laser shock forming of pure copper and titanium sheet with forming/blanking compound die," *Optics and Lasers in Engineering*, vol. 67, pp. 83–93, Apr. 2015, <https://doi.org/10.1016/j.optlaseng.2014.09.019>.
- [17] O. Hung, C. Chan, C. M. Yuen, and C. Kan, "8 - Application of laser technology," in *Sustainable Technologies for Fashion and Textiles*, R. Nayak, Ed. Woodhead Publishing, 2020, pp. 163–187.
- [18] F. Cheng, W. Ji, C. Qian, and J. Xu, "Cavitation bubbles dynamics and cavitation erosion in water jet," *Results in Physics*, vol. 9, pp. 1585–1593, Jun. 2018, <https://doi.org/10.1016/j.rinp.2018.05.002>.
- [19] C. Peng, S. Tian, G. Li, and M. C. Sukop, "Simulation of laser-produced single cavitation bubbles with hybrid thermal Lattice Boltzmann method," *International Journal of Heat and Mass Transfer*, vol. 149, Mar. 2020, Art. no. 119136, <https://doi.org/10.1016/j.ijheatmasstransfer.2019.119136>.
- [20] J. Gu, C. Luo, Z. Lu, P. Ma, X. Xu, and X. Ren, "Bubble dynamic evolution, material strengthening and chemical effect induced by laser cavitation peening," *Ultrasonics Sonochemistry*, vol. 72, Apr. 2021, Art. no. 105441, <https://doi.org/10.1016/j.ultsonch.2020.105441>.
- [21] G. Y. Yuan, B. Y. Ni, Q. G. Wu, Y. Z. Xue, and A. M. Zhang, "An experimental study on the dynamics and damage capabilities of a bubble collapsing in the neighborhood of a floating ice cake," *Journal of Fluids and Structures*, vol. 92, Jan. 2020, Art. no. 102833, <https://doi.org/10.1016/j.jfluidstructs.2019.102833>.

- [22] M. Xiang *et al.*, "Shock responses of nanoporous aluminum by molecular dynamics simulations," *International Journal of Plasticity*, vol. 97, pp. 24–45, Oct. 2017, <https://doi.org/10.1016/j.ijplas.2017.05.008>.
- [23] D. Errandonea and A. B. Garg, "Recent progress on the characterization of the high-pressure behaviour of AVO<sub>4</sub> orthovanadates," *Progress in Materials Science*, vol. 97, pp. 123–169, Aug. 2018, <https://doi.org/10.1016/j.pmatsci.2018.04.004>.
- [24] E.-A. Brujan, "Shock wave emission and cavitation bubble dynamics by femtosecond optical breakdown in polymer solutions," *Ultrasonics Sonochemistry*, vol. 58, Nov. 2019, Art. no. 104694, <https://doi.org/10.1016/j.ultsonch.2019.104694>.
- [25] K. Sato, Y. Sugimoto, and S. Ohjimi, "Pressure-wave formation and collapses of cavitation clouds impinging on solid wall in a submerged water jet," in *Proceedings of the 7th International Symposium on Cavitation CAV2009*, Ann Arbor, MI, USA, Aug. 2009.
- [26] H. Soyama, "Effect of nozzle geometry on a standard cavitation erosion test using a cavitating jet," *Wear*, vol. 297, no. 1, pp. 895–902, Jan. 2013, <https://doi.org/10.1016/j.wear.2012.11.008>.
- [27] N. V. Cuong and N. L. Khanh, "Parameter Selection to Ensure Multi-Criteria Optimization of the Taguchi Method Combined with the Data Envelopment Analysis-based Ranking Method when Milling SCM440 Steel," *Engineering, Technology & Applied Science Research*, vol. 11, no. 5, pp. 7551–7557, Oct. 2021, <https://doi.org/10.48084/etasr.4315>.
- [28] H. Takuda, T. Enami, K. Kubota, and N. Hatta, "The formability of a thin sheet of Mg–8.5Li–1Zn alloy," *Journal of Materials Processing Technology*, vol. 101, no. 1, pp. 281–286, Apr. 2000, [https://doi.org/10.1016/S0924-0136\(00\)00484-2](https://doi.org/10.1016/S0924-0136(00)00484-2).
- [29] L. Saidi, S. Mekroussi, S. Kherris, D. Zebbar, and B. Mébarki, "A Numerical Investigation of the Free Flow in a Square Porous Cavity with Non-Uniform Heating on the Lower Wall," *Engineering, Technology & Applied Science Research*, vol. 12, no. 1, pp. 7982–7987, Feb. 2022, <https://doi.org/10.48084/etasr.4604>.